

<b>Zeitschrift:</b>	Schweizerische mineralogische und petrographische Mitteilungen = Bulletin suisse de minéralogie et pétrographie
<b>Band:</b>	83 (2003)
<b>Heft:</b>	2
<b>Artikel:</b>	Pre-metamorphic $^{18}\text{O}$ signatures in morphologically complex zircons from the Qinglongshan UHP meta-granite (Sulu terrain, China)
<b>Autor:</b>	Giorgis, David / Rumble, Douglas / Cosca, Michael
<b>DOI:</b>	<a href="https://doi.org/10.5169/seals-63140">https://doi.org/10.5169/seals-63140</a>

### **Nutzungsbedingungen**

Die ETH-Bibliothek ist die Anbieterin der digitalisierten Zeitschriften auf E-Periodica. Sie besitzt keine Urheberrechte an den Zeitschriften und ist nicht verantwortlich für deren Inhalte. Die Rechte liegen in der Regel bei den Herausgebern beziehungsweise den externen Rechteinhabern. Das Veröffentlichen von Bildern in Print- und Online-Publikationen sowie auf Social Media-Kanälen oder Webseiten ist nur mit vorheriger Genehmigung der Rechteinhaber erlaubt. [Mehr erfahren](#)

### **Conditions d'utilisation**

L'ETH Library est le fournisseur des revues numérisées. Elle ne détient aucun droit d'auteur sur les revues et n'est pas responsable de leur contenu. En règle générale, les droits sont détenus par les éditeurs ou les détenteurs de droits externes. La reproduction d'images dans des publications imprimées ou en ligne ainsi que sur des canaux de médias sociaux ou des sites web n'est autorisée qu'avec l'accord préalable des détenteurs des droits. [En savoir plus](#)

### **Terms of use**

The ETH Library is the provider of the digitised journals. It does not own any copyrights to the journals and is not responsible for their content. The rights usually lie with the publishers or the external rights holders. Publishing images in print and online publications, as well as on social media channels or websites, is only permitted with the prior consent of the rights holders. [Find out more](#)

**Download PDF:** 27.01.2026

**ETH-Bibliothek Zürich, E-Periodica, <https://www.e-periodica.ch>**

# Pre-metamorphic $\delta^{18}\text{O}$ signatures in morphologically complex zircons from the Qinglongshan UHP meta-granite (Sulu terrain, China)

David Giorgis<sup>1\*</sup>, Douglas Rumble<sup>2</sup> and Michael Cosca<sup>1</sup>

## Abstract

Oxygen isotope analyses of bulk zircon grains and cores (isolated by air-abrasion) from ultra-high pressure (UHP) meta-granite from the Qinglongshan region of China, yield low  $\delta^{18}\text{O}$  values ranging from  $-0.2$  to  $-7.4\text{\textperthousand}$ . Sample characterization using back-scattered electron and cathodoluminescence techniques reveals inclusion-rich, morphologically complex zircon cores containing inclusions of biotite, quartz (no coesite as verified by Raman spectroscopy), K-feldspar, magnetite and apatite whereas the rims are inclusion-free. Allanite-(Ce) is compositionally heterogeneous with similar internal structures as the zircons. The allanite and the zircon cores are interpreted to have crystallized prior to UHP metamorphism within a fluid-rich environment. The mineral inclusions in zircon cores account for small  $\delta^{18}\text{O}$  differences (0.3 to  $1.0\text{\textperthousand}$ ) between abraded and non-abraded crystals. The pre-UHP metamorphic zircon cores probably acquired their negative  $\delta^{18}\text{O}$  values during Neoproterozoic sub-solidus crystallization in a magmatic hydrothermal system located in a cold climate environment.

**Keywords:** Meta-granite, allanite, zircon, oxygen isotopes, UHP rocks, hydrothermal system, Neoproterozoic.

## 1. Introduction and geological setting

Ultra-high pressure (UHP) rocks, including metabasalt, meta-granite and associated meta-sedimentary rocks from the Qinglongshan locality (Sulu terrain, eastern China) (Fig. 1A), were metamorphosed during the early Mesozoic collision of the North China and Yangtze Blocks (Li et al., 1993; Eide et al., 1994; Hacker and Wang, 1995; Ames et al., 1996; Chavagnac and Jahn, 1996; Rowley et al., 1997; Hacker et al., 1998; Zhang and Liou, 1998). These rocks have been intensively studied, in part because of their distinctive UHP parageneses and unusual “excess” argon and oxygen isotopic signatures (Li et al., 1994; Giorgis et al., 2000). Extremely low  $\delta^{18}\text{O}$  values ( $-15\text{\textperthousand}$  to  $-1\text{\textperthousand}$ ) have been reported for the UHP minerals by several authors (Yui et al., 1995; Zheng et al., 1996; Rumble and Yui, 1998) and interpreted as the result of meteoric water-rock interaction in a cold climate prior to Triassic (220–240 Ma) continental collision, subduction and UHP metamorphism.

Age estimates for protoliths of Qinglongshan eclogites indicate an upper intercept U–Pb age of

$762 \pm 28$  Ma for zircon (Ames et al., 1996). The Qinglongshan meta-granite, which is located 2 km south of the Qinglongshan locality (Fig. 1B), contains zircons whose cores have concordant  $^{238}\text{U}/^{206}\text{Pb}$  SHRIMP ages of 684 to 754 Ma (Rumble et al., 2002). The age of UHP metamorphism is given by mineral whole-rock isochrons as  $226.3 \pm 4.5$  Ma (Sm–Nd) and  $219.5 \pm 0.5$  Ma (Rb–Sr) (Li et al., 1994; Li, 1996). The lower discordia age of zircons from eclogite is  $217 \pm 9$  Ma (Ames et al., 1996). Rims of zircons from Qinglongshan meta-granite have  $^{238}\text{U}/^{206}\text{Pb}$  SHRIMP ages of 221 Ma (Rumble et al., 2002). These geochronological data are consistent with the hypothesis that Qinglongshan eclogite facies rocks represent the wall-rocks of the intrusive Qinglongshan meta-granite (Figs. 1A and 1B). To explain the low  $\delta^{18}\text{O}$  values, Rumble and Yui (1998) proposed that the Qinglongshan meta-granite was the heat source that drove convective circulation of ground water through meta-basalts and meta-sediments of the Qinglongshan wall-rocks.

To further understand this paleo-hydrothermal system, oxygen isotope analyses have been

<sup>1</sup> Institute of Mineralogy and Geochemistry, University of Lausanne, BFSH-2, CH-1015, Lausanne, Switzerland.  
[<dgiorgis@netcourier.com>](mailto:<dgiorgis@netcourier.com>)

<sup>2</sup> Geophysical Laboratory, 5251 Broad Branch Rd. N. W., Washington, D. C. 20015-1305, USA.

\* Present address: Ch. du Reposoir 5bis, 1007 Lausanne, Switzerland.

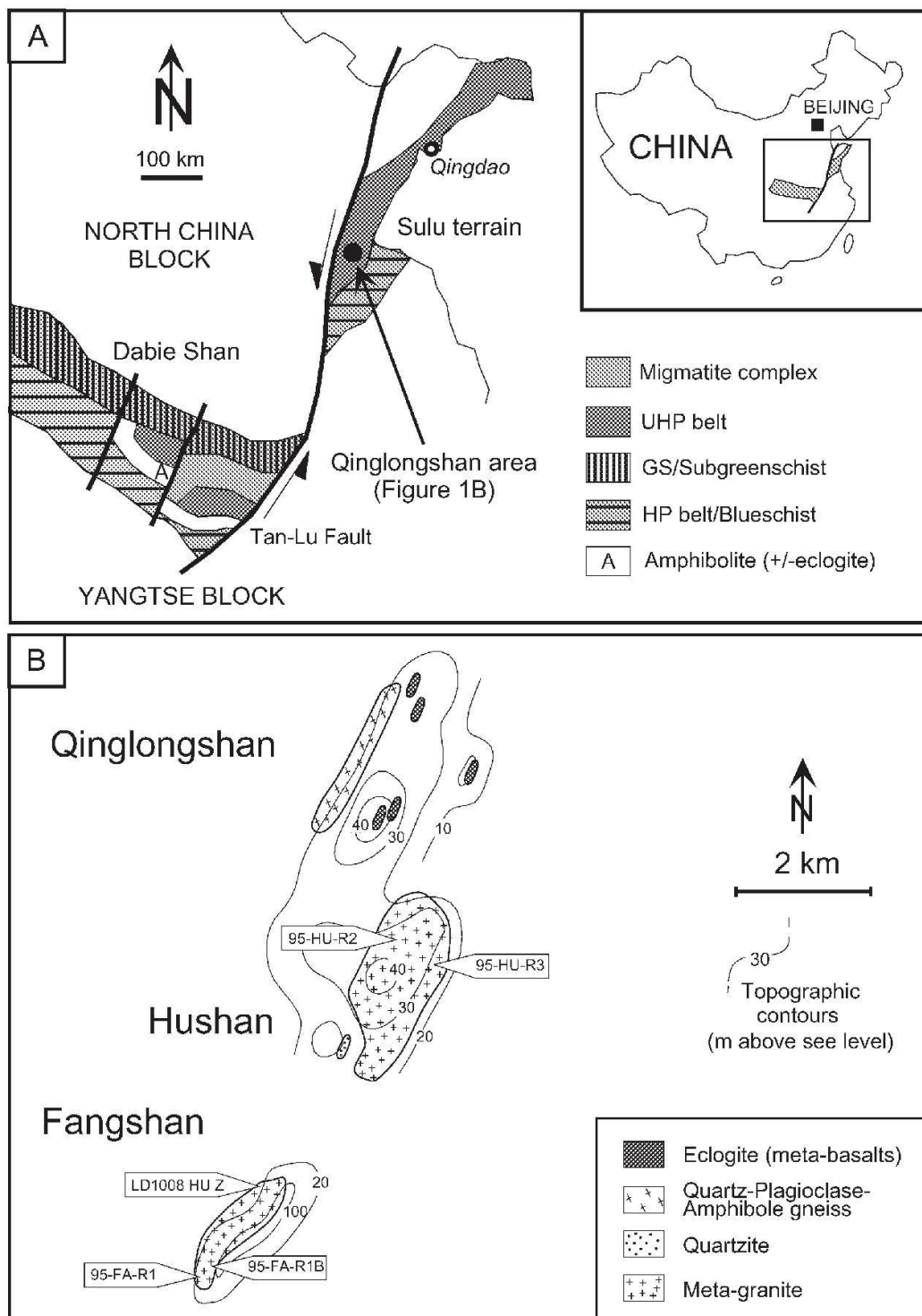


Fig. 1 (A) Sketch map of metamorphic belts of E. China, showing location of the Qinglongshan area. (B) Outcrop sketch map of the Qinglongshan area and sample location of the meta-granite (adapted from Rumble and Yui, 1998).

made on mineral separates of the Qinglongshan meta-granite (quartz, feldspar, biotite, magnetite, and garnet) with special attention placed on zircon. Zircon is a refractory mineral, which is extremely stable and resistant over a wide P-T range and is considered to be an excellent host for preserving UHP coesite or micro-diamond inclusions (Tabata et al., 1998). Recent studies have shown that zircon can record pre-metamorphic oxygen isotope information from metamorphosed magmatic rocks (Valley et al., 1994;

Watson and Cherniak, 1997; Peck et al., 2000). In this study, backscattered electron (BSE), cathodoluminescence (CL), and Raman microprobe analyses are used to demonstrate that the extremely negative  $\delta^{18}\text{O}$  values from cores and rims of zircons reveal oxygen isotopic signatures of pre-UHP metamorphic minerals. These data are interpreted within a context of a cold climate, magmatic hydrothermal system.

## 2. Petrographic features

The samples analyzed in this study were collected from an unweathered, weakly foliated meta-granite, which crops out over a distance of at least 7 km in quarries in Hushan and Fangshan (Fig. 1B). The exact nature of the protolith is unknown, but on the basis of mineralogic and petrographic characteristics, a granite, monzonite or a granodiorite is the most likely candidate. Mafic segregations occurring as lenses are common and contain variable amounts of titanite, hornblende (with biotite inclusions) and epidote.

The meta-granite contains an amphibolite-facies mineral assemblage of plagioclase, microcline, quartz, and biotite, with lesser garnet, epidote, and zoisite. Accessory minerals are magnetite, monazite, amphibole, titanite, allanite, and zircon. Rutile and coesite were not observed, but garnet, epidote, and omphacite (minerals often preserving coesite as inclusions) are uncommon in these rocks. With the exception of allanite and zircon, all minerals are presumed to have crystallized during Triassic UHP metamorphism.

Epidote ( $\text{Ps}_{27-36}$ ) commonly contains a core of allanite-(Ce) (Fig. 2C) and is interpreted as a pre-metamorphic igneous phase (Carswell et al., 1998; Liu et al., 1999). Skeletal garnet is rich in Mn and poor in Mg, which is typical of garnet from gneiss of the Dabieshan-Sulu region (Zhang et al., 1996). Rare phengite inclusions in plagioclase and from a whiteschist associated with the meta-granite have Si contents of  $\sim 3.4$  p.f.u., suggesting that the Qinglongshan meta-granite witnessed HP conditions. Biotite and epidote probably represent retrograde metamorphic phases, consistent with observations of Wang and Liou (1991), Okay (1993) and Liou et al. (1997), who considered these granitic gneisses as UHP rocks re-equilibrated at low-pressure conditions.

## 3. Analytical procedures

Oxygen isotope extraction was done using a  $\text{CO}_2$  laser fluorination system in the Geophysical Laboratory, similar to the setup of Sharp (1990). Mineral fractions of 1.5–2.5 mg have been used for

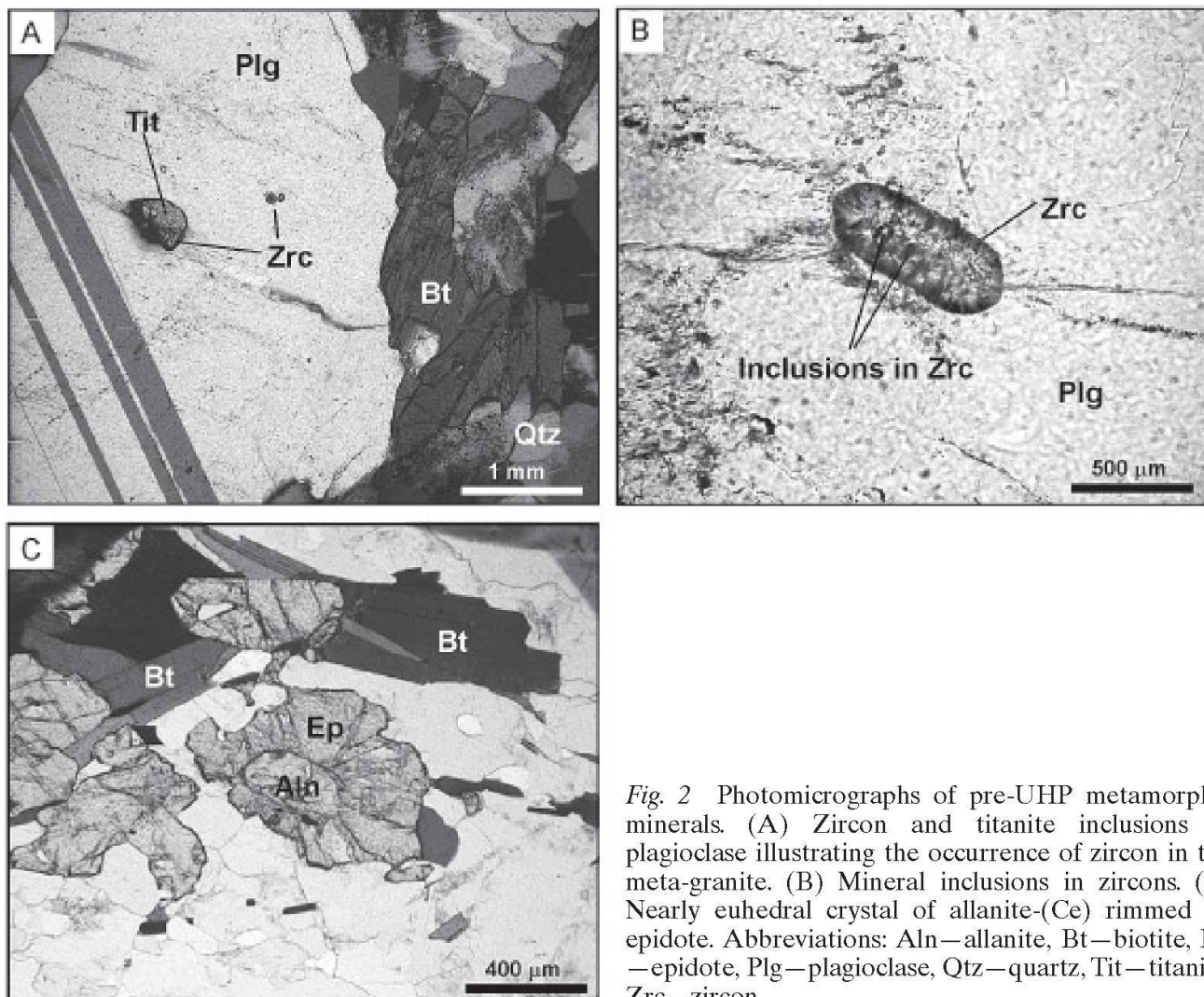


Fig. 2 Photomicrographs of pre-UHP metamorphic minerals. (A) Zircon and titanite inclusions in plagioclase illustrating the occurrence of zircon in the meta-granite. (B) Mineral inclusions in zircons. (C) Nearly euhedral crystal of allanite-(Ce) rimmed by epidote. Abbreviations: Aln—allanite, Bt—biotite, Ep—epidote, Plg—plagioclase, Qtz—quartz, Tit—titanite, Zrc—zircon.

Table 1  $\delta^{18}\text{O}_{\text{VSMOW}}$  values (‰) of minerals, mineral-mineral fractionations, and temperature estimates from the Qinglongshan meta-granite.

Sample	Mineral	$\delta^{18}\text{O}$ (‰)	$\delta^{18}\text{O}^*$ (‰)	Pairs	$\Delta^{18}\text{O}$ (‰)	T <sup>1</sup> (°C)	T <sup>2</sup> (°C)	T <sup>3</sup> (°C)	T <sup>4</sup> (°C)	T <sup>5</sup> (°C)
after air abrasion										
LD1008 Hu Z	Zircon	-5.9 <sup>#</sup>	-5.6 (30–35%)							
95-FA-R1	Quartz	0.6								
	Feldspar	-0.8		Qtz-Pl	1.4	602	623			
	Biotite	-4.9		Qtz-Bt	5.5	413	505			
	Magnetite	-7.4		Qtz-Mt	8.0	517				594
	Zircon	-2.4 <sup>#</sup>	-1.9 (20–30%)	Qtz-Zr	3.0					
95-HU-R3	Quartz	-4.2								
	Feldspar	-5.3		Qtz-Pl	1.1	735	738			
	Biotite	-8.1		Qtz-Bt	3.9	578	632			
	Zircon	-7.4 <sup>#</sup>	-7.1 (20–30%)	Qtz-Zr	3.2					
95-FA-R1B	Quartz	-1.0								
	Feldspar	-2.8		Qtz-Pl	1.8	473	517			
	Biotite	-6.6		Qtz-Bt	5.6	405	498			
	Magnetite	-9.5		Qtz-Mt	8.5	491				567
	Garnet	-5.3		Qtz-Grt	4.3	580			583	566
	Zircon	-5.7 <sup>#</sup>	-4.7 (10–15%)	Qtz-Zr	4.7					
95-HU-R2	Quartz	3.5								
	Feldspar	2.3		Qtz-Pl	1.2	686	695			
	Biotite	-1.4		Qtz-Bt	4.9	466	546			
	Zircon	-0.2 <sup>#</sup>	0.2 (20–30%)	Qtz-Zr	3.7					

<sup>1</sup> Temperature after Zheng (1991, 1993a,b)

<sup>2</sup> Temperature after Javoy (1977)

<sup>3</sup> Temperature after Rosenbaum and Matthey (1995)

<sup>4</sup> Temperature after Matthews (1994)

<sup>5</sup> Temperature after Clayton and Kieffer (1991)

\* Non-duplicated values. Percentage in bracket represents an estimate of air abraded zircon volume

<sup>#</sup> Whole grain analyses and abraded zircon data from Rumble et al. (2002)

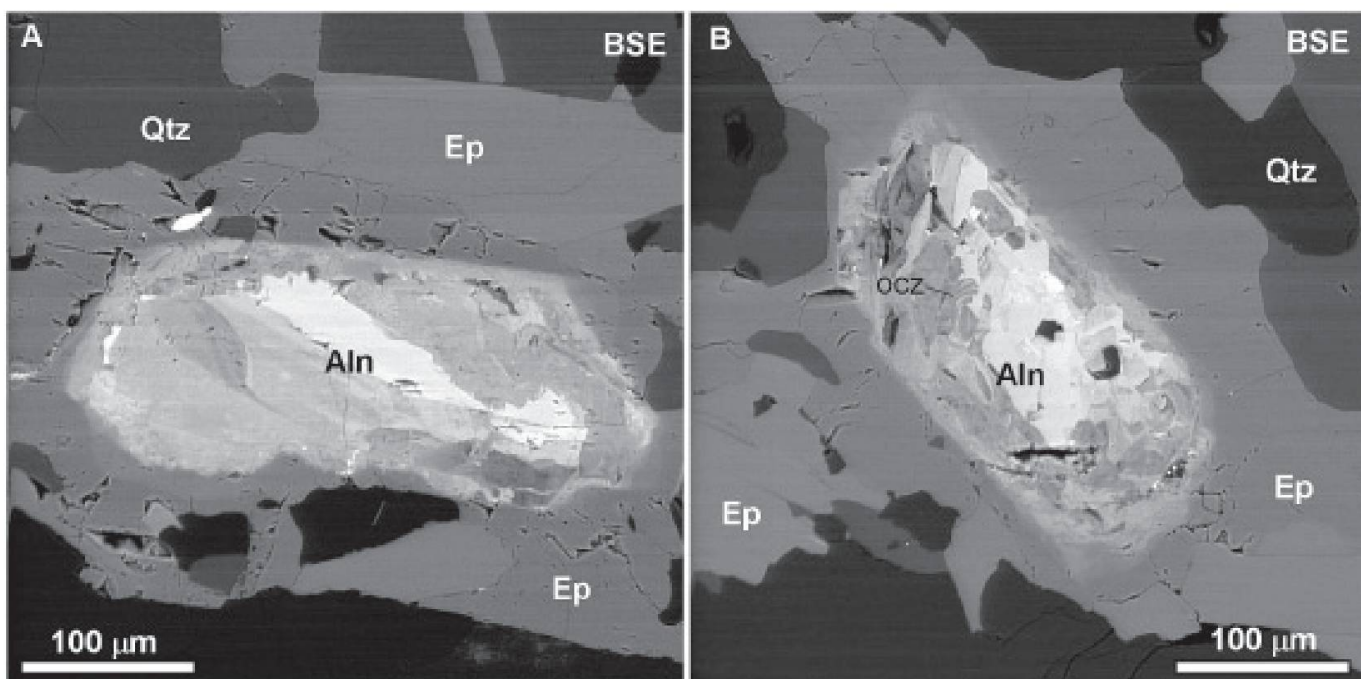


Fig. 3 (A and B) BSE images of epidote with allanite-(Ce) cores. Note preservation of idiomorphic allanite-(Ce) and complex internal structure due to a heterogeneous distribution of REE. Note also the fine-scale oscillatory zoning (ocz) in B. For abbreviations see Fig. 2.

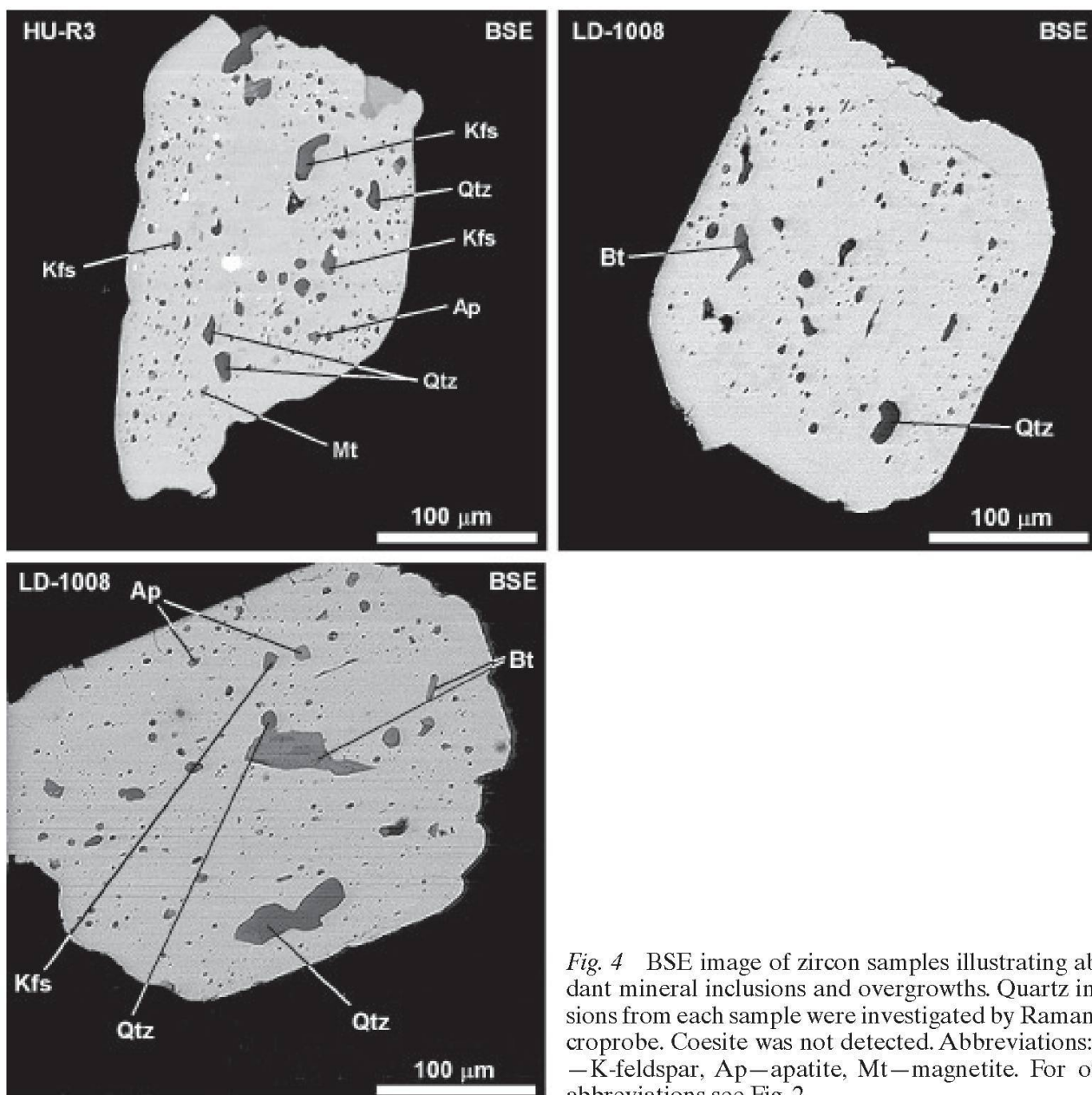


Fig. 4 BSE image of zircon samples illustrating abundant mineral inclusions and overgrowths. Quartz inclusions from each sample were investigated by Raman microprobe. Coesite was not detected. Abbreviations: Kfs—K-feldspar, Ap—apatite, Mt—magnetite. For other abbreviations see Fig. 2.

each analysis. Aliquots of oxygen isotope inter-laboratory reference material UWG-2 (garnet from Gore Mt. USA; Valley et al., 1995) were routinely analyzed with every loading of 12 samples and the data were standardized to its recommended  $\delta^{18}\text{O}$  value of +5.8‰. The reported  $\delta^{18}\text{O}$  values in Table 1 (apart from abraded zircons) are averages of duplicate or triplicate determinations with a precision of 0.1–0.2‰. A comparison of the  $\delta^{18}\text{O}$  values of air-abraded (Krogh, 1987) and non air-abraded zircon fractions was made in order to compare the oxygen isotopic signature of the core with zircon overgrowths (Table 1).

BSE and CL images were obtained using a Camscan SEM at the University of Lausanne on separated zircons impregnated in a low luminescent resin with accelerating voltages of 20 kV and 14 kV, respectively. Qualitative energy-dispersive

analysis (EDS) was employed to identify zircon inclusions. Raman microprobe analyses were made at the University of Geneva, using a Labram type Raman coupled with a He–Ne laser operating at a wavelength of 632.8 nm.

#### 4. Allanite

In the Qinglongshan meta-granite, allanite-(Ce) commonly preserves an idiomorphic habit with morphologically complex internal structures (see Fig. 3). Quantitative electron microprobe analyses (Giorgis, 2001) indicate that dark and bright zones observed in BSE images are due to variations in rare earth elements (REE). Zoning of REE is well documented in allanite from granitic rocks (Sorensen, 1991), and for allanite formed in

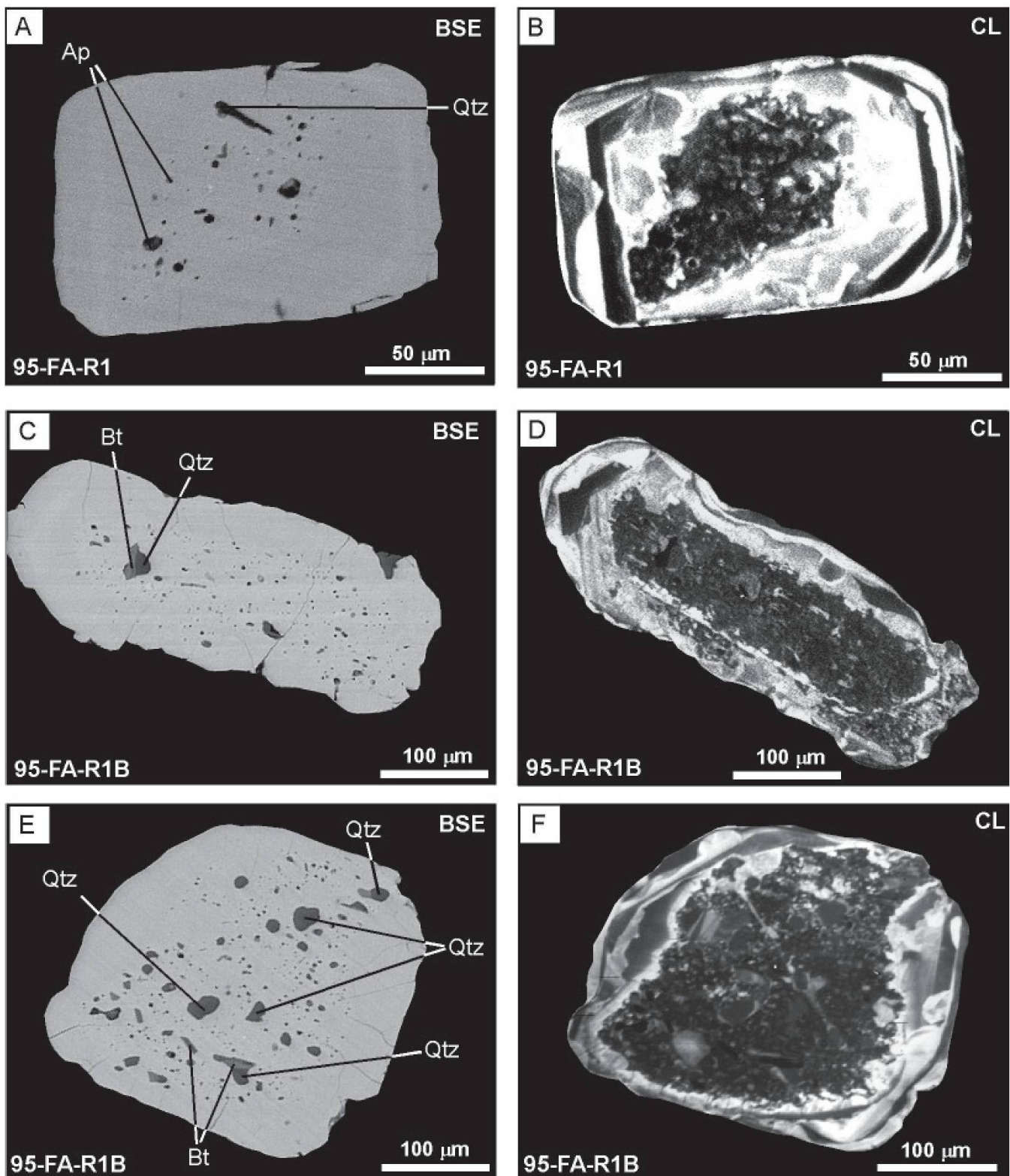


Fig. 5 (A-F) BSE and CL image pairs of zircon crystals showing cores containing mineral inclusions and complex internal morphologies. Rims are inclusion-free and display irregular patterns with some patchy zoning. In B, D and F, the boundary between the dark core and overgrowths shows embayments probably due to partial resorption. This boundary is surrounded by a bright rim. In Fig. 4F, rims (at the bottom right of the grain) might reflect recrystallization during metamorphism. For abbreviations see Figs. 2 and 3.

hydrothermal systems (Exley, 1980; Gromet and Silver, 1983; Sawka et al., 1984). Such zoning could be related to variations in fluid compositions or changes in REE contents of the melt during crystallization of allanite. However, in the Qinglongshan meta-granite, destabilization or partial disso-

lution of allanite-(Ce) during metamorphism and recrystallization could also explain the variable REE compositions. Some allanites contain fine-scale oscillatory zoning (Fig. 3B). Gromet and Silver (1983) observed sharp euhedral oscillatory zoning in a few allanite grains which they inter-

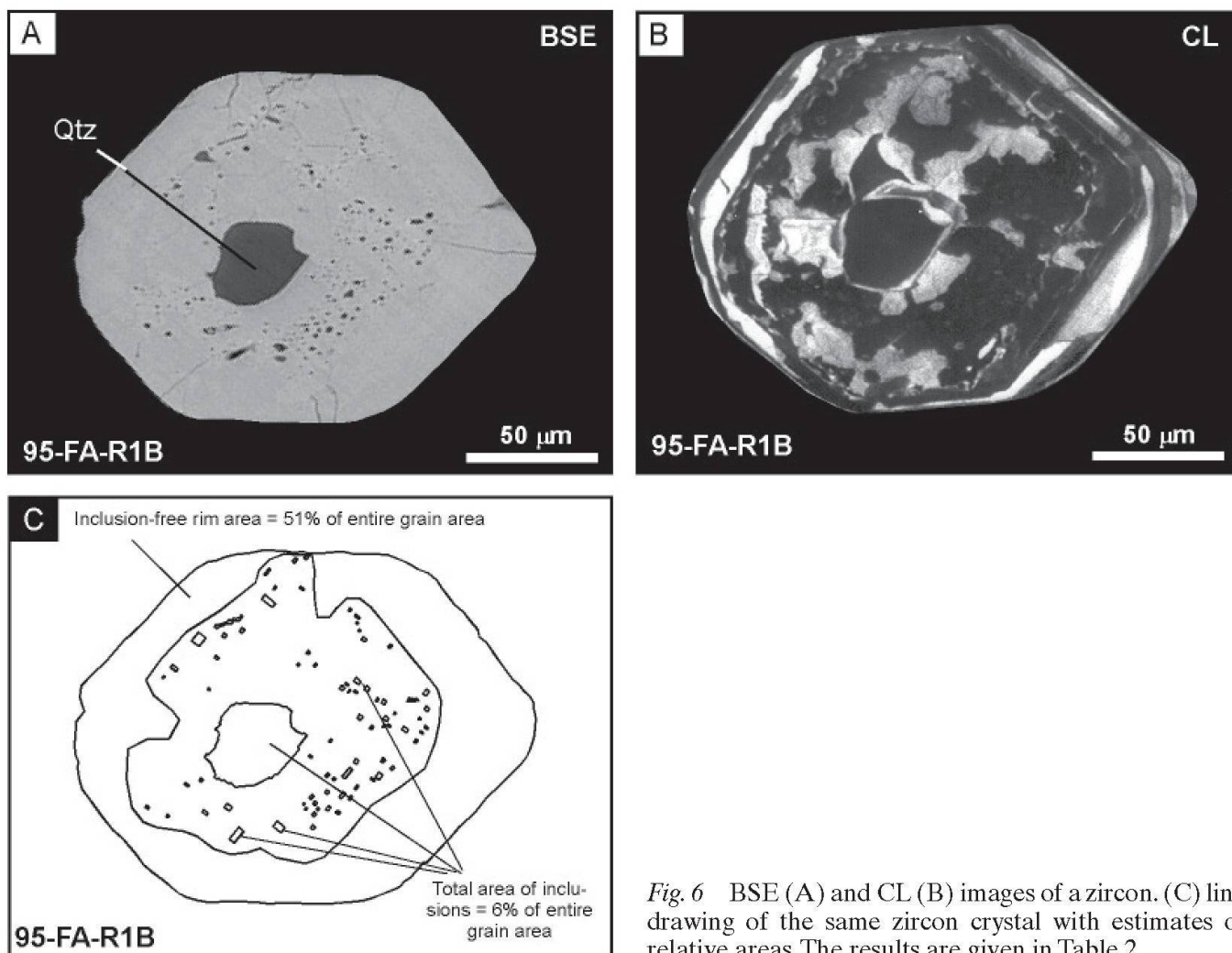


Fig. 6 BSE (A) and CL (B) images of a zircon. (C) line drawing of the same zircon crystal with estimates of relative areas. The results are given in Table 2.

preted as evidence for growth from a melt. However, Sorensen (1991) argued that such oscillatory zoning could also be related to sub-solidus growth.

### 5. Zircon

Zircon generally occurs as long (100–400 μm), weakly developed prisms in feldspar, biotite, and quartz (Fig. 2). The zircons cores are inclusion-rich, containing biotite, quartz, K-feldspar, magnetite and apatite (Figs. 4, 5A–E, 6A). A laser Raman microprobe was used to search for coesite, but quartz was the only  $\text{SiO}_2$  phase identified regardless of the size of the inclusions. No  $\text{SiO}_2$  inclusions were observed in the rims of the investigated zircons. CL images reveal zircon morphologies consistent with a multistage growth history (Figs. 5B, D, F, 6B). The zircon cores exhibit irregular sector zoning and amoeboid and chaotic internal structures without any oscillatory CL zoning. The zones with strong CL zoning correspond to the locations within the crystals where inclusions occur. The cores are surrounded by over-

growths (not observed in all zircons grains) that are free of inclusions and generally characterized by zones of irregular shape and patchy oscillatory zoning. The bright CL band between core and rims (Fig. 5B, D, F and 6B) show embayments, which could be the result of partial zircon resorption.

### 6. Oxygen isotope results

The  $\delta^{18}\text{O}$  values of quartz, feldspar, biotite, magnetite, and garnet range from +3.5 to −9.5‰, with significant heterogeneities observed between the different samples (Table 1). For example, samples 95-HU-R2 and 95-HU-R3 are from the Hushan outcrop but have very different  $\delta^{18}\text{O}$  values. Interestingly, the coexisting minerals in each meta-granite sample have nearly the same quartz-mineral fractionations, consistent with isotopic equilibrium (Fig. 7). Zircons have  $\delta^{18}\text{O}$  values ranging from −0.2 to −7.4‰, representing some of the most negative values ever recorded for zircons (Bindeman and Valley, 2000). The  $\delta^{18}\text{O}$  values obtained for each sample are reproducible, suggest-

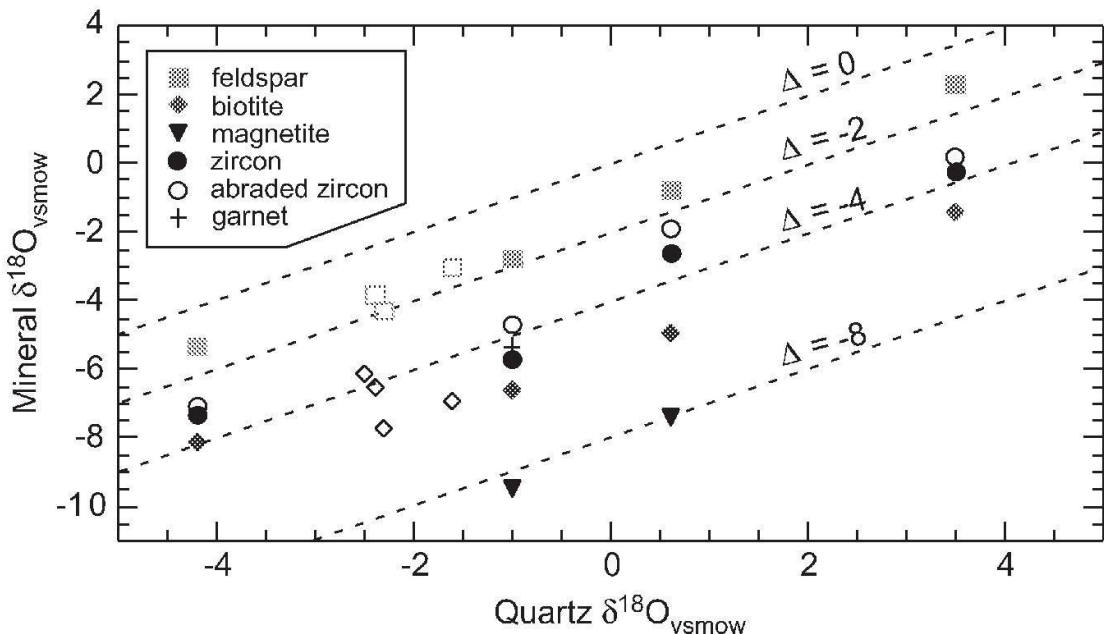


Fig. 7 Plot of oxygen isotope composition in various minerals vs. coexisting quartz in meta-granite from Qinglongshan. Open squares and open diamonds are from Rumble and Yui (1998). Zircon data from Rumble et al. (2002). All other data from this study.

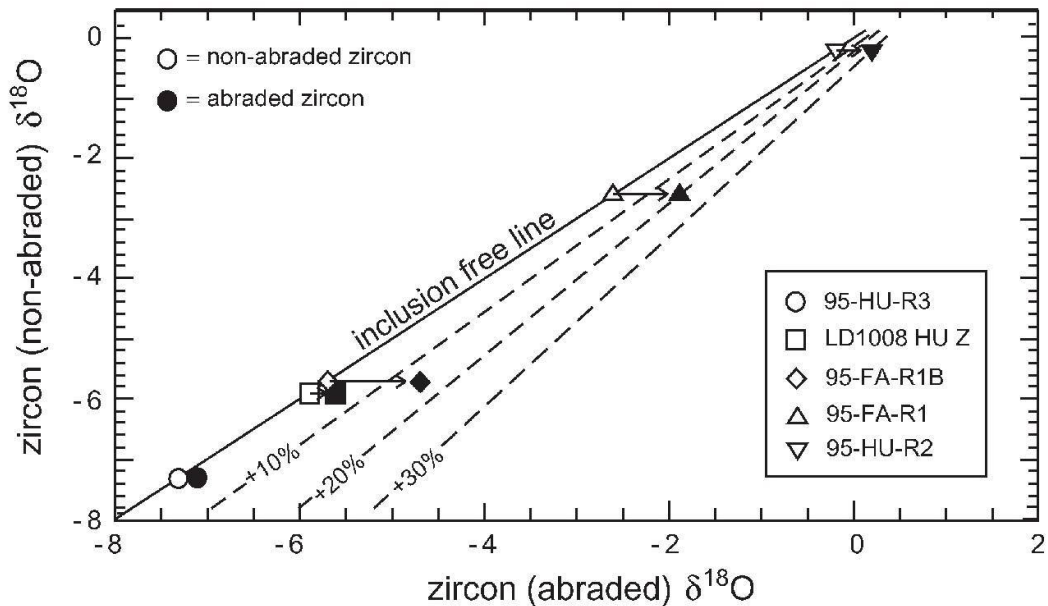


Fig. 8 Plot of  $\delta^{18}\text{O}$  values in zircon from non-abraded and abraded grains. Samples have slightly heavier  $\delta^{18}\text{O}$  values in the abraded grains, consistent with isotopically heavier inclusions located in zircon cores. Note that samples LD1008 HU Z, 95-HU-R3 and 95-HU-R2 have the smallest volume proportion of rim overgrowths (Table 2) and have the smallest  $\delta^{18}\text{O}$  differences between abraded and non-abraded grains (see text for further explanation). Dashed lines correspond to various percentage of inclusions. We assume that (1)  $\delta^{18}\text{O}$  values of zircon rims =  $\delta^{18}\text{O}$  values of zircon cores, and (2)  $\delta^{18}\text{O}$  values of inclusions = +1 (arbitrary value).

ing that the number and the nature of the inclusions are quite similar between the different individual zircon grains and that broken crystals probably have a minor influence on the  $\delta^{18}\text{O}$  values. The  $\delta^{18}\text{O}$  values obtained for the abraded grains are 0.3 to 1.0‰ heavier than the whole grains (Table 1), due to the variable modal abundance of the isotopically heavier inclusions.

## 7. Oxygen isotope thermometry

Metamorphic temperatures were calculated for the Qinglongshan meta-granite using the stable isotope results (Table 1). Except for the quartz-garnet pairs, empirical calibrations from Zheng (1991, 1993a and 1993b) yield temperatures that are systematically lower than temperatures ob-

tained using calibrations of Javoy (1977) and Clayton and Kieffer (1991). The oxygen isotope thermometry results show significant inter-sample variation, especially when comparing fast oxygen-diffusing minerals such as magnetite and biotite. These results are consistent with variable diffusional re-equilibration and cannot be interpreted with any certainty. Rumble and Yui (1998) also suggested caution in applying isotope thermometry in these UHP rocks. Nevertheless, the range in mineral fractionations observed in the present investigation are similar to those of Rumble and Yui (1998) for Qinglongshan eclogites. This observation is consistent with the interpretation that the Qinglongshan meta-granite had a similar metamorphic history to the associated eclogitic rocks.

If zircon overgrowths crystallized during UHP metamorphism they should be in oxygen isotopic equilibrium with the garnet. For a temperature of 800 °C, Valley et al. (1994) suggest a garnet-zircon fractionation of 0.0. This implies that in sample 95-FA-R1B (the only sample with metamorphic garnet), the  $\delta^{18}\text{O}$  values of zircon overgrowths should be similar to those of garnet. Indeed, the stable isotope data are qualitatively consistent with this hypothesis, as the  $\delta^{18}\text{O}$  value of the garnet (−5.3) is between lower  $\delta^{18}\text{O}$  values for the bulk zircon (−5.7) and higher  $\delta^{18}\text{O}$  values for the abraded zircon (−4.7). In addition, systematic fractionations between some of the other coexisting minerals including quartz-zircon, and feldspar-zircon suggest that isotopic equilibrium was approached, if not attained (Fig. 7).

## 8. Effects of inclusions in zircons

To evaluate the importance of rim overgrowths and inclusions in zircons on their  $\delta^{18}\text{O}$  values, the volume proportion of each of these domains was estimated using BSE and CL images with AutoCAD Map® software for image analysis. Because of the irregular shape of the zircons and their cross sections in BSE, we chose not to impose geometric constraints for these calculations and instead simply assume that the proportions determined in two dimensions are equally appropriate over the volume of the mineral grain (Fig. 6C). The results are given in Table 2. Estimations from the image analysis indicate overgrowths represent between 0 and 50% of the total zircon. In rare instances, overgrowths can represent up to 70% of the zircon (Fig. 5A), but this is probably due to uncompensated 3D effects. One risk of assuming that rim and inclusion proportions estimated from two dimensional images can be ap-

plied over the volume of the crystal may be that we overestimate the percentage of rims and underestimate the percentage of inclusions. Consequently, the volume proportions of rims and inclusions indicated in Table 2 are thought to be maximum and minimum estimates, respectively.

The difference in  $\delta^{18}\text{O}$  values between abraded and non-abraded grains (Table 1) can be interpreted to reflect either the effect of inclusions or differences in the  $\delta^{18}\text{O}$  signature of zircon cores versus rims, or a combination of both. Inclusions (mainly quartz, plagioclase and biotite) are estimated to represent between 0 and 6 vol% of the total zircon, and between 0 and 12 vol% of the abraded zircons (Table 2). Calculations have been made using these volume proportions together with several assumed  $\delta^{18}\text{O}$  values for inclusions (mainly quartz and plagioclase), in order to estimate the average  $\delta^{18}\text{O}$  values of the inclusion-free cores and rims. Assuming that inclusions have an average  $\delta^{18}\text{O}$  value between 0 and 3‰ heavier than that of zircon, consistent with the data in Table 1, values of inclusion-bearing cores are estimated to be about 0.2 and 1.0‰ heavier than the inclusion-free rims. Thus, it appears that in addition to the minor effects that inclusions have on the overall  $\delta^{18}\text{O}$  values of the zircons, small but noticeable differences in the  $\delta^{18}\text{O}$  values exist between the cores and rims of the zircons. Accepting the oxygen diffusion parameters by Watson and Cherniak (1997), it should not be possible to homogenize the  $\delta^{18}\text{O}$  values between zircon cores and rims by diffusion during UHP metamorphism. Consequently, zircon cores are interpreted to record low  $\delta^{18}\text{O}$  values that were acquired prior to UHP metamorphism. This low  $\delta^{18}\text{O}$  signature not only survived conditions of UHP metamorphism, but the coexisting minerals in the meta-granites such as quartz, feldspar, and biotite also acquired correspondingly low  $\delta^{18}\text{O}$  values during UHP metamorphism and retrograde history because of limited isotopic exchange with an external isotopic reservoir (Fig. 7).

## 9. Discussion

The absence of coesite in the zircons, the lack of fluid circulation during UHP metamorphism (Liou and Zhang, 1996; Liou et al., 1997; Rumble and Yui, 1998), and the late Proterozoic  $^{238}\text{U}/^{206}\text{Pb}$  zircon ages obtained from the meta-granite (Rumble et al., 2002) indicate that zircon cores represent old (pre-UHP metamorphic) relics from the protolith. Furthermore, the elastic models of Gillet et al. (1984) and Van der Molen and Van Roermund (1986) suggest that quartz inclu-

Table 2 Volume proportion estimates of cores, rims, and inclusions in different zircon grains.

Sample	Mineral	vol%		vol%		vol% zircon (less inclusions)
		rim (inclusion free)	core	inclusions in core	inclusions in entire grain	
LD1008 Hu Z	Zircon 1	19.3	80.7	5.8	4.7	95.4
	Zircon 2	no rims	100.0	6.3	6.3	93.7
	Zircon 3	no rims	100.0	8.5	8.5	91.5
	Zircon 4	no rims	100.0	10.5	10.5	89.5
	Zircon 5	no rims	100.0	6.9	6.9	93.1
95-FA-R1	Zircon 1	65.0	35.0	4.4	1.5	98.5
	Zircon 2	59.4	40.6	5.0	2.0	98.0
	Zircon 3	68.1	31.9	5.0	1.6	98.4
95-HU-R3	Zircon 1	no rims	100.0	6.4	6.4	93.6
	Zircon 2	no rims	100.0	10.0	10.0	90.0
	Zircon 3	no rims	100.0	6.7	6.7	93.3
95-FA-R1B	Zircon 1	48.8	51.2	11.4	5.8	94.2
	Zircon 2	50.1	49.9	4.8	2.4	97.6
	Zircon 3	no rims	100.0	8.2	8.2	91.8
	Zircon 4	38.8	61.2	10.4	6.4	93.6
	Zircon 5	47.7	52.3	6.5	3.4	96.6

Volume proportions are assumed to equal area proportions. No estimates have been made for sample 95-HU-R2.

sions located in the inherited core of the zircons cannot be transformed to coesite during prograde UHP metamorphism. Such observations are in agreement with a pre-UHP metamorphic origin for the core of zircons. The overall irregular pattern of the zircon rims is typical for metamorphic zircon (Rubatto and Gebauer, 2000), which could be related to the UHP metamorphism, although the absence of mineral inclusions (especially coesite) in these overgrowth zones make it difficult to test this hypothesis. In addition, resorption observed at the boundary between core and rim overgrowths are probably due to the UHP metamorphism. Moreover, both zircon and allanite have significant variations in REE concentrations at the sub-grain scale, suggesting that both minerals originally crystallized prior to UHP metamorphism.

The  $\delta^{18}\text{O}$  heterogeneities between the different zircon cores are significant (+0.2‰ and -7.1‰ for samples 95-HU-R2 and 95-HU-R3, respectively) and consistent with the variations recorded by other coexisting minerals in these samples. These heterogeneities are interpreted as pre-metamorphic. The absence of magmatic oscillatory zoning in the zircon cores is evidence that the zircons did not crystallize from a typical magma. Localized heterogeneity in  $\delta^{18}\text{O}$  is known from unmetamorphosed hydrothermal systems where it is attributed to incomplete equilibration between heated meteoric waters circulating through a fracture network and the wall-rocks (Sheppard and Taylor, 1974). The inclusions concentrated in the zircon cores are furthermore consistent with a

subsolidus environment, and the geochronological data suggest the inclusions were incorporated during zircon growth between 684 to 754 Ma (Rumble et al., 2002), probably within a high-level magmatic system with large-scale hydrothermal circulation. One possible environment promoting such subsolidus zircon crystallization could occur in the regions affected by near surface hydrothermal fluids circulating in proximity to a cooling intrusion. Although the environment in which these zircons crystallized is enigmatic, the low zircon  $\delta^{18}\text{O}$  values are consistent with crystallization in the presence of high fluid activity where rocks interacted differentially with meteoric water (e.g., Friedman et al., 1974; Hildreth et al., 1984). These relationships lead us to speculate as to a possible geological environment that could produce the observed textures and oxygen isotope values. Isotopically zoned zircons with low  $\delta^{18}\text{O}$  values have been reported from the Yellowstone magmatic system (Bindeman and Valley, 2000), and demonstrate that such features may not be unusual. What is unusual in the Qinglongshan meta-granite are the low  $\delta^{18}\text{O}$  values recorded in all of the minerals, including zircon, providing strong evidence that the meteoric waters with which they interacted were of cold climate (Rumble et al., 2002).

## 10. Conclusions

Pre-metamorphic  $\delta^{18}\text{O}$  heterogeneities in zircon cores, together with chaotic internal structures in

zircon cores and allanite-(Ce) are consistent with a scenario in which zircons and allanites crystallized in a fluid-rich environment with a low  $^{18}\text{O}/^{16}\text{O}$  imposed by a meteoric fluid. Such an environment is consistent with the paleo-hydrothermal system proposed by Rumble et al. (2002) to explain the very negative  $\delta^{18}\text{O}$  values recorded in the UHP metamorphic rocks of the Qinglongshan area. Furthermore, these data are in agreement with Rumble and Yui (1998) and Rumble et al. (2002), that the Qinglongshan meta-granite is a reasonable candidate for the heat source of the Qinglongshan hydrothermal system. Oxygen isotope signatures of quartz, feldspar, biotite, magnetite, garnet, and oxygen isotope thermometry indicate that the Qinglongshan meta-granite had a similar metamorphic history to the surrounding UHP rocks. These data also suggest that, similar to the Qinglongshan meta-basalts and meta-sediments, oxygen isotopic exchange was strongly limited (at the meter scale) during UHP metamorphism. Not only are pre-metamorphic  $\delta^{18}\text{O}$  signatures preserved in zircon cores, but zircon rims, quartz, biotite, feldspar, magnetite, and garnet that crystallized during UHP conditions also inherited the low  $\delta^{18}\text{O}$  values of the protolith because of the limited scale of isotopic exchange.

### Acknowledgements

We thank Xu Huifen, Yang Jingsui, Zhang Zeming, and Xu Zhiqin for the mineral separations made at the Chinese Academy of Geological Science, Beijing and for assistance in the field, and to Dr. Robert Moritz (University of Geneva) for technical and scientific support during the Raman investigation. This study was supported by the Swiss National Science Foundation (grants 2100-049410.96 and 2000-65025.01). J.G. Liou and R.Y. Zhang provided support in the field. We gratefully acknowledge the support of NSF grant EAR-9526700, the David and Lucile Packard Foundation, and the US-China cooperative research project NSF EAR 98-14468. We are grateful to Z.D. Sharp and Y. Shieh for their reviews and comments, and we thank L.P. Baumgartner, C.P. Chamberlain, J.G. Liou, K. Mezger, and R.Y. Zhang for contributing to the study through discussion and criticism. The many editorial suggestions of R. Gieré greatly improved the presentation of this manuscript and are very much appreciated.

### References

Ames, L., Zhou, G. and Xiong, B. (1996): Geochronology and isotopic character of ultrahigh-pressure metamorphism with implications for collision of the Sino-Korean and Yangtze cratons, central China. *Tectonics* **15**, 472-489.

Bindeman, I.N. and Valley, J.W. (2000): Formation of low- $\delta^{18}\text{O}$  rhyolites after caldera collapse at Yellowstone, Wyoming, USA. *Geology* **28**, 719-722.

Carswell, D.A., Wilson, R.N. and Zhai, M. (1998): The enigma of eclogite-gneiss relationship in the ultra-high pressure terrane of Dabieshan, central China. *Intern. Workshop on UHP metamorphism and exhumation (abst.)*, Stanford Univ., A40-44.

Chavagnac, V. and Jahn, B.M. (1996): Coesite-bearing eclogites from the Bixiling Complex, Dabie Mountains, China: Sm-Nd ages, geochemical characteristics and tectonic implications. *Chem. Geol.* **133**, 29-51.

Clayton, R.N. and Kieffer, S.W. (1991): Oxygen isotopic thermometer calibrations. In: Taylor, H.P., O'Neil, J.R. and Kaplan, I.R. (eds.): *Stable Isotope Geochemistry: A tribute to Samuel Epstein*, The Geochemical Society, Special Publication no. **3**, 3-10.

Eide, E., McWilliams, M. and Liou, J. (1994):  $^{40}\text{Ar}/^{39}\text{Ar}$  geochronology and exhumation of high-pressure to ultrahigh-pressure metamorphic rocks in east-central China. *Geology* **22**, 601-604.

Exley, R.A. (1980): Microprobe studies of REE-rich accessory minerals: implications for Skye granite petrogenesis and REE mobility in hydrothermal systems. *Earth Planet. Sci. Lett.* **48**, 97-110.

Friedman, I., Lipman, P.W., Obradovich, J.D., Gleasen, J.D. and Christiansen, R.L. (1974): Meteoric water in magmas. *Sciences* **184**, 1069-1072.

Gillet, P., Ingrin, J. and Chopin, C. (1984): Coesite in subducted continental crust: P-T history deduced from elastic model. *Earth Planet. Sci. Lett.* **70**, 426-436.

Giorgis, D. (2001): Radiogenic and stable isotopic study of metamorphic rocks: case studies from Qinglongshan UHP rocks (Sulu terrain, China) and the Isorsuua complex (southern West Greenland). Unpubl. Ph.D. thesis, University of Lausanne, 150 pp.

Giorgis, D., Cosca, M. and Li, S. (2000): Distribution and significance of extraneous argon in UHP eclogite (Sulu terrain, China): insight from in situ  $^{40}\text{Ar}/^{39}\text{Ar}$  UV-laser analysis. *Earth Planet. Sci. Lett.* **181**, 605-615.

Gromet, L.P. and Silver, L.T. (1983): Rare earth element distributions among minerals in a granodiorite and their petrogenetic implications. *Geochim. Cosmochim. Acta* **47**, 925-939.

Hacker, B.R. and Wang, Q. (1995): Ar/Ar geochronology of ultrahigh-pressure metamorphism in central China. *Tectonics* **14**, 994-1006.

Hacker, B.R., Ratschbacher, L., Webb, L., Ireland, T., Walker, D. and Dong, S. (1998): U/Pb zircon ages constrain the architecture of the ultrahigh-pressure Qinling-dabie Orogen, China. *Earth Planet. Sci. Lett.* **161**, 215-230.

Hildreth, W., Christiansen, R.L. and O'Neil, J.R. (1984): Catastrophic isotopic modification of rhyolitic magma at times of caldera subsidence, Yellowstone Plateau Volcanic Field. *J. Geophys. Res.* **89**, 8339-8369.

Jahn, B.M. (1998): Geochemical and isotopic characteristics of UHP eclogites and ultramafic rocks of the Dabie Orogen: Implications for continental subduction and collisional tectonics. In: Hacker, B.R. and Liou, J.G. (eds.): *When Continents Collide: Geodynamics and Geochemistry of Ultrahigh-Pressure Rocks*. Kluwer Academic Publishers, Dordrecht, 203-239.

Javoy, M. (1977): Stable isotopes and geothermometry. *J. Geol. Soc. London* **133**, 609-636.

Krogh, T.E. (1987): Improved accuracy of U-Pb zircon ages by the creation of more concordant systems using an air abrasion technique. *Geochim. Cosmochim. Acta* **46**, 637-649.

Li, S., Xiao, Y., Zhang, Z., Chen, Y., Sun, S.-S., Cong, B., Liu, D., Ge, N., Hart, S.R. and Zhang, R. (1993): Collision of the North China and Yangtze Blocks and formation of coesite-bearing eclogites: Timing and processes. *Chem. Geol.* **109**, 89-11.

Li, S., Wang, S., Chen, Y., Liu, D., Qiu, J., Zhou, H. and Zhang, Z. (1994): Excess Ar in phengite from eclogite: Evidence from dating of eclogite minerals by Sm–Nd, Rb–Sr, and  $^{40}\text{Ar}/^{39}\text{Ar}$  methods. *Chem. Geol.* **112**, 343–350.

Li, S. (1996): Isotopic geochronology. In: Cong, B. (ed.): Ultrahigh-Pressure Metamorphic Rocks in the Dabie-Sulu Region of China. Science Press Kluwer Academic Publishers, Beijing, Dordrecht, 90–105.

Liou, J.G. and Zhang, R.Y. (1996): Occurrences of intergranular coesite in ultrahigh-P rocks from the Sulu region, eastern China: Implication for lack of fluid during exhumation. *Am. Mineral.* **81**, 1217–1221.

Liou, J.G., Zhang, R.Y. and Ernst, W.G. (1997): Lack of fluid during ultrahigh-P metamorphism in the Dabie-Sulu region, eastern China. In: Proceedings of 30th International Geological Congress. VSP Scientific Publisher Netherland, 17, 141–156.

Liou, K., Dong, S., Xue, H. and Zhou, J. (1999): Significance of allanite-(Ce) in granitic gneisses from the ultrahigh-pressure metamorphic terrane, Dabie Shan, central China. *Mineral. Mag.* **63**, 579–586.

Matthews, A. (1994): Oxygen isotope geothermometers for metamorphic rocks. *J. Metamorphic Geol.* **12**, 211–219.

Okay, A. and Sengör, A.M.C. (1993): Tectonics of an ultrahigh-pressure terrane: The Dabie Shan/Tongbai Shan orogen, China. *Tectonics* **12**, 1320–1334.

Peck, W.H., King, E.M. and Valley, J.W. (2000): Oxygen isotope perspective on Precambrian crustal growth maturation. *Geology* **28**, 363–366.

Rosenbaum, J.M. and Matthey, D. (1995): Equilibrium garnet-calcite oxygen isotope fractionation. *Geochim. Cosmochim. Acta* **59**, 2839–2842.

Rowley, D.B., Xue, F., Tucker, R.D., Peng, Z.X., Baker, J. and Davis, A. (1997): Ages of ultrahigh pressure metamorphism and protolith orthogneisses from the eastern Dabie Shan: U/Pb zircon geochronology. *Earth Planet. Sci. Lett.* **151**, 191–203.

Rubatto, D. and Gebauer, D. (2000): Use of cathodoluminescence for U–Pb zircon dating by ion microprobe: Some examples from the Western Alps. In: Pagel, M., Barbin, V., Blanc, P. and Ohnenstetter, D. (eds.): Cathodoluminescence in Geosciences. Springer Verlag, Heidelberg, 373–400.

Rumble, D. and Yui, T.-F. (1998): The Qinglongshan oxygen and hydrogen anomaly near Donghai in Jiangsu Province, China. *Geochim. Cosmochim. Acta* **62**, 3307–3322.

Rumble, D., Giorgis, D., Ireland, T., Zhang, Z., Xu, H., Yui, T.F., Yang, J., Xu, Z. and Liou, J.G. (2002): Low  $\delta^{18}\text{O}$  zircons, U/Pb dating, and the age of the Qinglongshan oxygen and hydrogen isotope anomaly near Donghai in Jiangsu Province, China. *Geochim. Cosmochim. Acta* **66**, 2299–2306.

Sawka, W.N., Chappel, B.W. and Norrish, K. (1984): Light-rare-earth-element zoning in sphene and allanite during granitoid fractionation. *Geology* **12**, 131–134.

Sharp, Z. (1990): A laser-based microanalytical method for the in situ determination of oxygen isotope ratios of silicates and oxides. *Geochim. Cosmochim. Acta* **54**, 1353–1357.

Sheppard, S.M.F. and Taylor, H.P. jr. (1974): Hydrogen and oxygen isotope evidence for the origin of water in the Boulder batholith and the Butte ore deposits. *Econ. Geol.* **69**, 926–946.

Sorensen, S. (1991): Petrogenetic significance of zoned allanite in garnet amphibolites from a paleo-subduction zone: Catalina Schist, southern California. *Am. Mineral.* **76**, 589–601.

Tabata, H., Yamauchi, K. and Maruyama, S. (1998): Tracing the extent of a UHP metamorphic terrane: Mineral-inclusion study of zircons in gneisses from the Dabie Shan. In: Hacker, B.R. and Liou, J.G. (eds.): When Continents Collide: Geodynamics and Geochemistry of Ultrahigh-Pressure Rocks. Kluwer Academic Publishers, Dordrecht, 261–273.

Valley, J.W., Chiarenzelli, J.R. and McLellan, J.M. (1994): Oxygen isotope geochemistry of zircons. *Earth Planet. Sci. Lett.* **126**, 187–206.

Valley, J.W., Kitchen, N., Kohn, M.J., Niendorf, C.R. and Spicuzza, M.J. (1995): UWG-2, a garnet standard for oxygen isotope ratios. Strategies for high precision and accuracy with laser heating. *Geochim. Cosmochim. Acta* **59**, 5223–5231.

Van der Molen, I. and Van Roermund, H.L.M. (1986): The pressure path of solid inclusions in minerals: the retention of coesite inclusions during uplift. *Lithos* **19**, 317–324.

Wang, X. and Liou, J.G. (1991): Regional ultrahigh-pressure metamorphic terrane in central China: evidence from coesite bearing eclogite, marble and metapelite. *Geology* **19**, 933–936.

Watson, E.B. and Cherniak, D.J. (1997): Oxygen diffusion in zircon. *Earth Planet. Sci. Lett.* **148**, 527–544.

Yui, T.F., Rumble, D. and Lo, C.H. (1995): Unusually low  $\delta^{18}\text{O}$  ultra-high-pressure metamorphic rocks from the Sulu Terrain, eastern China. *Geochim. Cosmochim. Acta* **59**, 2859–2864.

Zhang, R., Liou, J.G. and Kai, Y. (1996): Petrography of UHPM rocks and their country rock gneisses. In: Cong, B. (ed.): Ultrahigh-Pressure Metamorphic Rocks in the Dabie-Sulu Region of China. Kluwer Academic Publishers, Dordrecht, 49–68.

Zhang, R.Y. and Liou, J.G. (1998): Ultrahigh-pressure metamorphism of the Sulu terrane, Eastern China: prospective view. *Continental Dynamics* **3**, 32–53.

Zheng, Y.F. (1991): Calculation of oxygen isotope fractionation in anhydrous silicate minerals. *Geochim. Cosmochim. Acta* **57**, 1079–1091.

Zheng, Y.F. (1993a): Calculation of oxygen isotope fractionation in metal oxides. *Geochim. Cosmochim. Acta* **55**, 2299–2307.

Zheng, Y.F. (1993b): Calculation of oxygen isotope fractionation in hydroxyl-bearing silicates. *Earth Planet. Sci. Lett.* **120**, 247–263.

Zheng, Y.F., Fu, B., Gong, B. and Li, S. (1996): Extreme  $^{18}\text{O}$  depletion in eclogite from the Su-Lu terrane in east China. *Eur. J. Mineral.* **8**, 317–323.

Received 17 September 2002

Accepted in revised form 18 July 2003

Editorial handling: R. Gieré